ARTICLE

Pore-Filling Nanoporous Templates from Degradable Block Copolymers for Nanoscale Drug Delivery

Kuan-Hsin Lo,[†] Mei-Chin Chen,[‡] Rong-Ming Ho,[†,*] and Hsing-Wen Sung[†,*]

[†]Department of Chemical Engineering, National Tsing Hua University, Hsinchu 30013, Taiwan, and [‡]Department of Chemical Engineering, National Cheng Kung University, Tainan City 701, Taiwan

ABSTRACT Nanoporous thin-film samples, fabricated from degradable block copolymers, polystyrene-*b*-poly(L-lactide) (PS—PLLA), were utilized as templates for the formation of ordered nanoarrays. This work elucidates the feasibility of using such nanoporous PS templates as coatings on implantable devices for drug delivery through pore-filling sirolimus. Specific pore-filling process was adopted to increase loading efficiency by exploiting the capillary force associated with the tunable wetting property of the sirolimus solution. After the pore-filling process, sirolimus-loaded cylindrical and lamellar nanoarrays can be obtained. A comparison with those of macroscale templates indicates that the developed nanoporous templates can successfully entrap the loaded drug in nanoscale pores, markedly increasing the duration of drug delivery. As a result, the size, geometry, and depth of the nanoscale pores of the nanoporous templates can be readily controlled to regulate the drug release profiles.

KEYWORDS: nanoporous material · template · degradable block copolymer · nanoscale drug delivery · implantable device

The self-assembly of soft matter, both organic and biological materials, is one of the most convenient means of creating nanostructures with various functions and complexity. The self-assembled morphologies from block copolymers (BCPs) satisfy the size requirement for nanotechnological applications. The self-assembly of BCPs that is driven by the incompatibility of constituent blocks can be exploited to fabricate nanomaterials with controlled geometries and unique functions. Accordingly, nanostructures prepared by the self-assembly of BCPs, in particular nanostructured thin films, are ideal templates for the formation of nanostructured hybrids and nanocomposites.[1−10]

BCP thin-film samples with nanoporous textures can be obtained by chemically removing one block using UV,[11] oxygen plasma,[12] ozone exposure,[4] and base aqueous solution.[9,13] The nanoporous thin films can be exploited as templates so as to fabricate various nanostructured hybrids and nanocomposites *via* the pore-filling process to generate novel nanomaterials with practical applications. Russell and co-workers successfully applied BCP templates with nanoporous patterns to orient tri-*n*-octylphosphine oxide (TOPO)-covered CdSe nanoparticles by the capillary force.[14] Hillmyer and co-workers demonstrated that ordered nanoporous monoliths could be filled with water-soluble materials to yield large aspect ratios in monolithic nanoporous polymer frameworks.[15,16] In our previous studies, a successful pore-filling process in nanoporous polystyrene (PS) templates from degradable BCPs was developed for hybridization by exploiting the capillary force associated with the tunable wetting property of the precursor solution. Consequently, CdS nanocrystals could be *in situ* generated by exposing the BCP template incorporated with cadmium acetate ($CdAc_2$) to H_2S vapor.[17] Also, a straightforward and effective method for fabricating patterned CNT nanoarrays has been developed by electroplating for Ni deposition so as to serve as catalytic nanoarrays for the growth of CNTs.[10]

This work aims to elucidate the feasibility of using nanoporous PS templates for the controlled release of drugs through pore-filling sirolimus into the templates. PS is widely applied in cell culture applications because of its nontoxicity, and sirolimus is a potent immunosuppressive agent with anti-inflammation and antiproliferation characteristics.[18,19] Also, a unique block copolymer system, poly(styrene-*b*-isobutylene-*b*-styrene) (SIBS), has been used successfully as the carrier for a drug-eluting coronary stent (Boston Scientific's TAXUS stent) because of its hemocompatibility and biocompatibility.[20] In fact, many organic approaches have been developed for the sustained release of drugs loaded in various systems, such as core/shell nanospheres,[21]

*Address correspondence to rmho@mx.nthu.edu.tw, hwsung@che.nthu.edu.tw.

Received for review March 26, 2009 and accepted August 07, 2009.

Published online August 21, 2009.
10.1021/nn900299z CCC: $40.75

mesoporous silica nanoparticles,[22] and polymer nanoparticles.[23] In platform applications, a titania nanotube template that is fabricated on an implant surface can be loaded with antibiotics to prevent bacterial infection.[24,25] However, a consistent limitation of these local delivery methods is the rapid loss of therapeutic agents from the implant within hours or even minutes of their being administered. To solve this problem, nanoporous PS templates which can be applied to the implant surface for the sustained delivery of therapeutic agents locally in a nanoscale drug-eluting manner are used, and the results of their use are investigated. The formation of sirolimus-loaded nanoarrays is exploited to achieve a surprisingly extended drug-eluting duration, indicating that nanoscale control markedly affects the diffusion property of drug elution, suggesting a new methodology for controlled elution.

RESULTS AND DISCUSSION

A template that was composed of nanoporous thin film was prepared from degradable BCPs, and a supporting ion-coated metallic substrate that simulated an implant surface was used. A series of degradable BCPs, polystyrene-*b*-poly(L-lactide) (PS−PLLA), was synthesized.[26,27] A template with large-scale oriented cylindrical nanochannels from the self-assembly of PS−PLLA was obtained by nanopatterning and hydrolysis.[9,10] Since the template on glass substrate can easily cause delamination and breakage of the film during the hydrolytic process, the film was exposed to UV radiation with a wavelength of 254 nm under vacuum for more than 10 min to increase the mechanical strength and the adhesion of the template.[28] Owing to the degradable character of the polyester component,[13] the hydrolysis of the PS−PLLA thin film provides a simple method of preparing a nanoporous template for the pore-filling process. A specific pore-filling process, shown in Scheme 1, was designed to increase the pore-filling efficiency. For the wetting ability of capillary force, a solution of sirolimus was prepared by dissolving it in a mixed solvent of ethanol and water. Considering the adhesion and application, the template was removed from the glass substrate using 1% HF solution, and then floated onto the solution surface for the pore-filling of the sirolimus, and finally collected by gold-coated substrate. After drying in air overnight, the sirolimus-loaded template was immersed in the test tubes and incubated in a water-bath shaker to investigate the drug eluting profile.[29]

Figure 1 displays the transmission electron microscopic (TEM) images of the nanoporous template and sirolimus-loaded nanoarrays through the pore-filling process driven by directed capillary force. As shown in Figure 1a and

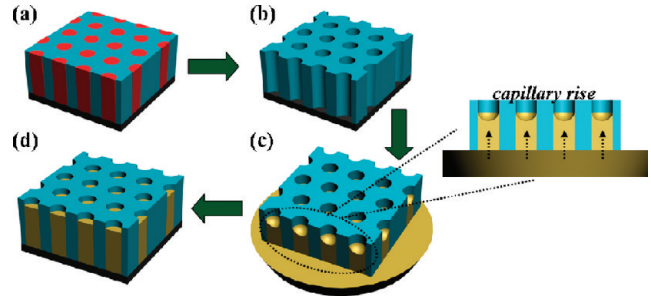

Scheme 1. Schematic illustration of pore-filling process by directed capillary force: (a) PS−PLLA thin film; (b) nanoporous PS template from hydrolytic PS−PLLA thin film; (c) nanoporous PS template floated onto the surface of solution for pore-filling sirolimus; (d) templated sirolimus nanoarrays from pore-filling template.

Figure 1c, hexagonally packed cylindrical and lamellar nanochannel arrays can be obtained following the hydrolytic process at which the PS template appears as gray matrix and the nanopores and nanochannels are both bright regions because of the mass−thickness contrast. After the pore-filling process, the templated sirolimus was negatively stained by potassium phosphotungstate (PTA). Because of the hydrogen bond between sirolimus and PTA, significant dark sirolimus nanoarrays dispersed in the gray PS matrix can be clearly observed in Figure 1b and Figure 1d. Furthermore, the diameter of the sirolimus-loaded cylindrical nanoarrays is approximately equal to the size of the pores in the nanoporous templates, indicating that the sirolimus is indeed introduced into the oriented cylindrical nanochannels *via* the pore-filling process.

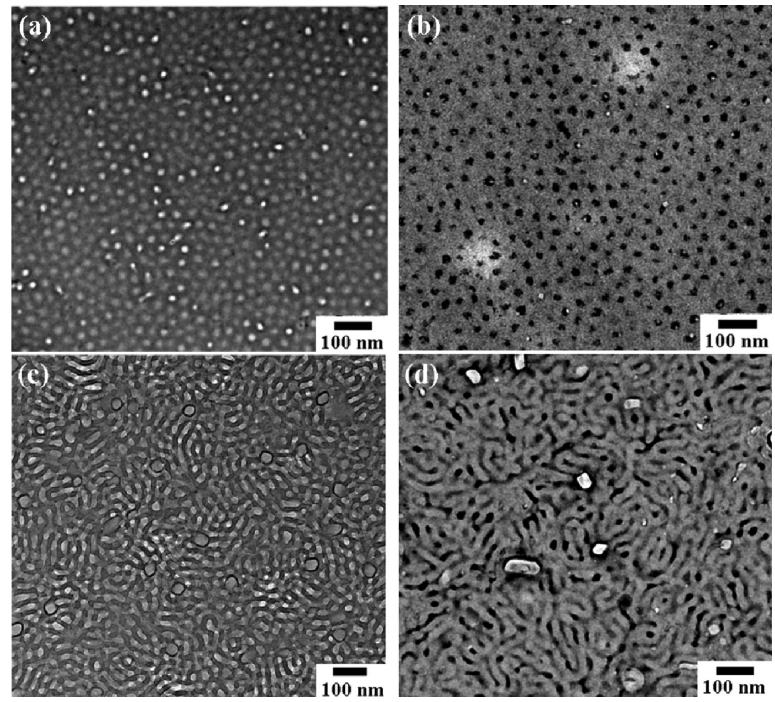

Figure 1. TEM images of (a) cylindrical nanoporous PS template from hydrolytic PS−PLLA thin film; (b) sirolimus-loaded cylindrical nanoarrays from pore-filling template; (c) lamellar nanochannel PS template from hydrolytic PS−PLLA thin film; (d) sirolimus-loaded lamellar nanoarrays from pore-filling template.

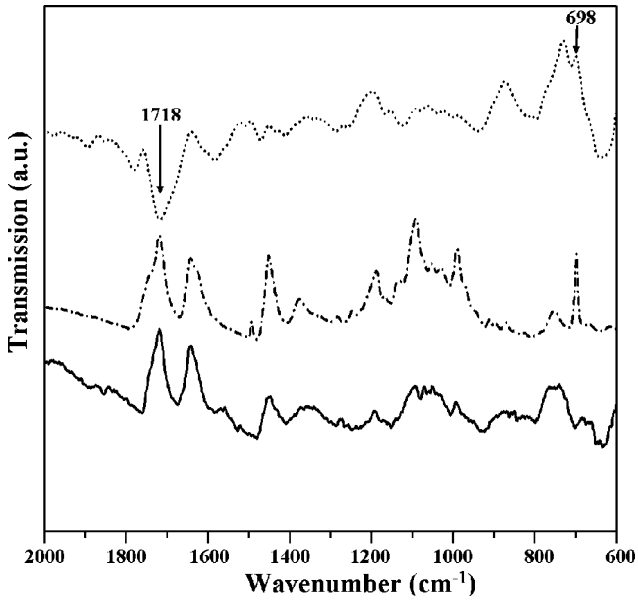

Figure 2. FTIR spectra of PS template whose pores are filled with sirolimus before (dash-dot line) and after (dot line) drug elution. The solid line represents the spectrum of pure sirolimus.

To verify the presence of the templated-sirolimus nanoarrays, attenuated total reflection Fourier transform infrared (ATR-FTIR) spectroscopy was applied to identify the chemical absorption of sirolimus. The solid line in Figure 2 reveals the pure sirolimus material, whose characteristic absorption peak at 1718 cm^{-1} corresponds to the deformation mode of the sirolimus C═O. In contrast, the dash dot line in Figure 2 represents the spectrum of sirolimus-loaded cylinderical nanoarrays, with an absorption peak at 698 cm^{-1} corresponding to the C−H bond on the benzene ring of PS, whereas the absorption peak characteristic of sirolimus at 1718 cm^{-1} can be also clearly identified, revealing the presence of the templated sirolimus after the pore-filling process. After drug elution, the FTIR includes only the absorption peak of PS at 698 cm^{-1} (dot line) and the sirolimus peak at 1718 cm^{-1} disappears, suggesting successful elution in the water-bath shaker.

Figure 3 shows the results of *in vitro* drug elution from the sirolimus-loaded cylindrical and lamellar nanoarrays; those obtained from the anodized aluminum oxide (AAO)/sirolimus hybrids and the PS/sirolimus blends were used as controls. Notably, the AAO/sirolimus hybrids possessed cylindrical pores with a diameter of about 200 nm, and the prepared PS/sirolimus blends exhibited phase separation on the micrometer scale. The release profiles from the AAO/sirolimus hybrids and the PS/sirolimus blends revealed the fast release of the drug with an initial burst effect. In contrast, the drug-release profile observed from the sirolimus-loaded cylindrical nanoarrays exhibited no burst release; instead, a prolonged and sustained-release profile was observed. For example, after a 15 h release, the cumulative amounts of drug eluted from the AAO/sirolimus hybrids and the PS/sirolimus blends were approximately 70% and 60%, respectively, indicating inadequate retention of the loaded sirolimus. In contrast, for the sirolimus-loaded cylindrical and lamellar nanoarrays, the cumulative amount of eluted drug was reduced markedly to 30% and 37%; the period of sustained-release of sirolimus was 10 days. Note that the thickness of the sirolimus-loaded cylindrical and lamellar nanoarrays used herein was only 60 nm. The duration of drug elution may be further prolonged by increasing the thickness of the sirolimus-loaded cylindrical nanoarrays *via* an appropriate pore-filling process. The error bars on the data obtained from the sirolimus-loaded cylindrical nanoarrays were significantly smaller than those from the AAO/sirolimus hybrids and the PS/sirolimus blends. We suggest that the unique elution profile of the sirolimus-loaded cylindrical nanoarrays is attributed to the nanoscale size effect on the controlled release of drugs. Since the sirolimus-loaded cylindrical nanoarrays were made from the cylindrical nanochannels (20 nm in diameter), the sirolimus was effectively entrapped, resulting in a well-controlled specific releasing profile. The drug-elution results for the sirolimus-loaded lamellar nanoarrays (with a lamellar microdomain width of 20 nm) revealed a similar nanosize effect; the duration of sustained release also reached 10 days. Furthermore, the templates with various thicknesses were prepared to ex-

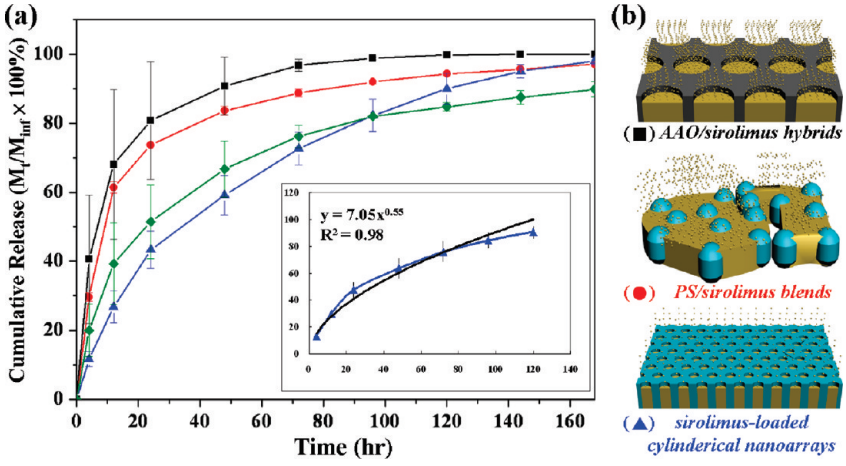

Figure 3. (a) Cumulative release profiles of sirolimus from sirolimus-loaded cylindrical nanoarrays (blue triangle), sirolimus-loaded lamellar nanoarrays (green diamond), AAO/sirolimus hybrids (black square), and PS/sirolimus blends (red circle). Inset plots the fitted curve (black line) for the release profile of sirolimus-loaded cylindrical nanoarrays. M_{inf} is the infinite amount of loaded drugs in test templates; M_t is the cumulative amount of drug released at time *t*. (b) Schematic illustration of the sirolimus-loaded cylindrical nanoarrays, the AAO/sirolimus hybrids, and the PS/sirolimus blends.

amine the thickness effect on the releasing amount of drug elution. As illustrated in Figure 4, the drug loading content (LC) of the sirolimus-loaded nanoarrays increases with increasing its thickness. Therefore, it is reasonable to observe that the total amount of drug elution is notably affected by the thickness of the sirolimus-loaded nanoarrays (see Table 1).

In contrast to the nanoscale size effect on the drug elution, it is also noted that the adsorption/desorption process for the loaded sirolimus within the template may play the role for the drug-elution. As reported by Hillmyer and co-workers, the hydroxyl groups on the internal surface of the pores could be obtained after the hydrolysis of PS-PLA.[30] Nevertheless, the density of the polar groups is not high enough to have a significant effect on the pore surface properties.[16] Moreover, the native AAO membrane also possesses the hydroxyl groups on the internal surface of the pores,[31] but no significant increase on releasing time in the AAO case could be found. As a result, the adsorption/desorption process that depends on the hydrophilicity of the template plays an insignificant role with respect to the endurance of the drug-elution.

To study the unique drug-elution profile associated with nanoscale delivery, the release profiles were fitted by a semiempirical power law,[32]

$$\frac{M_t}{M_{inf}} = kt^n \qquad (1)$$

where M_t is the cumulative amount of drug released at time t; M_{inf} is the cumulative amount of drug released at infinite time; M_t/M_{inf} is the fraction of the drug eluted; t is time; k is a characteristic constant of the system; n is the release exponent related to the mechanism of drug-elution. As presented in the inset of Figure 3, the equation for the drug-elution profile is similar to Higuchi equation ($n = 0.55$, $R^2 = 0.98$, except at the last stage of release), reflecting the fact that the release of sirolimus from the templated sirolimus nanoarrays is a diffusion-controlled process.[32] We suggest that the unique release profile of the sirolimus-loaded nanoarrays is attributed to the nanoscale size effect on the controlled release of drugs that changes the releasing mechanism. A diffusion-control process can be achieved by using sirolimus pore-filling template with tens nanometer size, whereas burst releasing is encountered once the pore size of the template is over hundreds nanometers. Similar behavior has also been observed recently by Desai and co-workers.[33] They fabricated a series of titanium dioxide (TiO_2) arrays with various lengths and diameters. The changes in drug delivery observed with variations in nanotube dimensions and lengths are in line

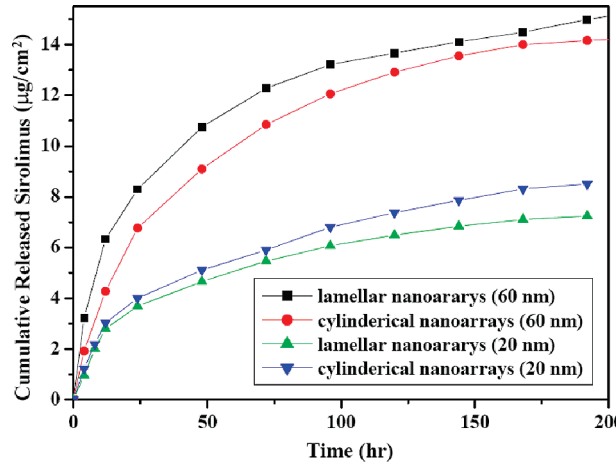

Figure 4. Cumulative release profiles of sirolimus released from test nanoarrays in different thicknesses.

with the hypothesis that the nanoscale size effect changes the releasing mechanism so as to affect the drug-elution behavior profoundly.

Sirolimus can inhibit the proliferation of vascular smooth muscle cells by blocking cell cycle progression at the G_1/S transition.[34] To evaluate the activity of the sirolimus that was released from the cylindrical or lamellar nanoarrays, rat thoracic aorta smooth muscle cells (RASMC) were treated for 3 days with a collected medium that contained the sirolimus released from the cylindrical or lamellar nanoarrays. A live/dead viability kit, containing calcein-AM and ethidium homodimer, was adopted to distinguish between live and dead cells.[35] Calcein-AM penetrates the cytosol of viable cells and stains them green, while ethidium homodimer stains dead cell nuclei red.[35] The cell viabilities of RASMC that had been treated with the fresh medium and those that had been treated with the collected media were visualized by fluorescence microscopy (Figure 5). The cell viability of RASMC was significantly reduced by treatment with the collected media because of the release of sirolimus; the antiproliferative activities of the sirolimus released from these two nanoarrays on RASMC were comparable.

CONCLUSION

A highly ordered sirolimus-loaded template in nanoscale was prepared and its characteristic elution profile for the release of drugs was obtained, suggesting that the nanoporous template has an

TABLE 1. Loading Contents (LC) of the Cylindrical Nanoarrays and the Lamellar Nanoarrays in Different Thicknesses

thickness	20 nm	40 nm	60 nm
cylinderical nanoarrays (μg/cm²)	7.2	12.9	16.1
lamellar nanoarrays (μg/cm²)	8.5	10.9	14.3

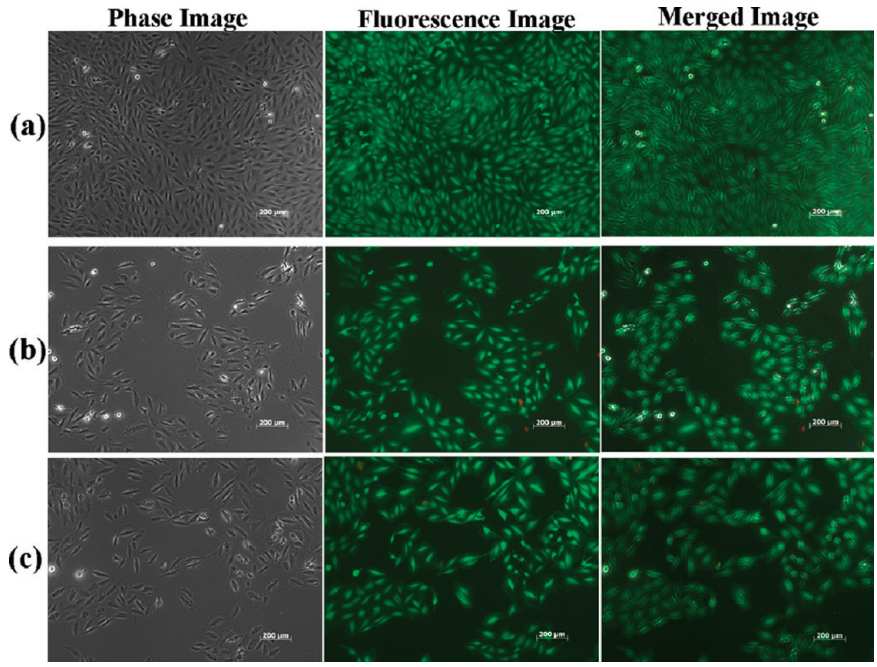

Figure 5. Results of activity assay of sirolimus released from cylindrical or lamellar nanoarrays. Fluorescence microscopic images, showing viability of RASMC following treatment for 3 days with (a) fresh medium or collected medium that contained the sirolimus that was released from the (b) cylindrical or (c) lamellar nanoarrays.

appealing application as a drug-elution coating on implantable devices. To be therapeutically effective, a useful drug delivery system must deliver a certain amount of drug over an extended period. The results of *in vitro* drug elution demonstrated that the developed template can successfully entrap the loaded drug in nanoscale pores for sustained release. As a result, the size, geometry, and depth of the nanoscale pores in the developed template can be readily controlled to regulate the drug release profiles to meet the specific requirements in clinical applications.

EXPERIMENTAL SECTION

PS−PLLA diblock copolymers with PLLA volume fraction of 0.25 and 0.48 were prepared by two-step living polymerization in sequence. The PS homopolymer was obtained by free radical polymerization of styrene, producing hydroxyl-terminated polystyrene as the macroinitiator. The ring-opening polymerization of L-lactide was then performed in the presence of the macroinitiator.[26,27] A thin-film sample with perpendicular cylindrical or lamellar nanostructures was initially formed onto glass substrate by spin-coating from a 1.5 wt % chlorobenzene solution of PS−PLLA at 1000 rpm, a 1.0 wt % solution of PS−PLLA at 1000 rpm and 3000 rpm at 50 °C. Samples with different film thicknesses, approximately 60, 40, and 20 nm, could be obtained. The thin-film thickness was determined by scanning probe microscopy (SPM), and the measurement details were described in the Supporting Information. Table 2 presents the characteristics of the samples. The gel permeation chromatography (GPC) measurements were performed on a Hitachi L-7100 system equipped with a differential Bischoff 8120 RI detector using THF (HPLC grade) as an eluent. Molecular weight and molecular weight distributions were calculated using polystyrene as standard. The number average molecular weight (M_n) of 4-hydrolysis-TEMPO terminated PS and polydispersity (PDI) of PS−PLLA block copolymer were obtained by GPC analysis. The molecular weight of PLLA blocks was measured by ^{1}H NMR analysis. On the basis of molecular weight and volume ratio, these PS−PLLAs (Table 2) are designated as PS*x*−PLLA*y* ($f_{PLLA}{}^v = z$);. *x* and *y* represent the numbers of repeating units for PS and PLLA blocks measured by NMR, respectively, and *z* indicates the volume fraction of PLLA calculated by assuming densities of PS and PLLA are 1.02 and 1.248 g/cm^3.

After it has been dried in a vacuum overnight, the film was exposed to UV radiation (wavelength at 254 nm) under a vacuum for over 10 min. The thin-film sample was then placed in NaOH solution for 5 days to degrade PLLA, and finally dispersed in MeOH solution to wash out residual degradation solution. For use in the pore-filling process, a 5 wt % solution of sirolimus was prepared by dissolving it into ethanol and water. The sirolimus (Rapamycin) was obtained from LC Laboratories (Woburn, MA). The control was commercially obtained AAO membranes, with an average diameter and thickness of 200 nm and 60 μm, respectively. Following the successful procedure for pore-filling agents by using AAO membrane,[36,37] several drops of 5 wt % sirolimus solution in ethanol and water were placed onto a glass substrate. An AAO membrane was immediately placed on the top of the solution, and then the nanopores of the membrane were filled with the sirolimus solution within seconds by capillary force. After solvent evaporation at ambient conditions, the pore-filled AAO membrane was dispersed in ethanol solution to wash out residual sirolimus on the surface so as to form the AAO/sirolimus hybrids. The PS/sirolimus blends were formed on Au-coated substrate by spin-coating (1000 rpm) from a tetrahydro-

TABLE 2. Characterists of PS−PLLA Block Copolymers

	M_n, PS [g/mol][a]	M_n, PLLA [g/mol][b]	PDI[a]	$f_{PS}{}^v$	morphology
S38−L16	38200	15700	1.21	0.75	cylinder
S14−L15	13600	15300	1.16	0.52	lamellar

[a]Measured from GPC analysis. [b]Obtained from integration of ^{1}H NMR measurement.

furan solution of 1.0 wt % 33700 g/mol PS homopolymer and 5 wt % sirolimus.

After drying in a vacuum overnight, the aforementioned distinct templates, loaded with sirolimus, were individually immersed in test tubes that contained sterilized phosphate buffered saline (PBS, pH 7.4) and incubated in a water-bath shaker at 37 °C at 120 rpm.[29] The incubated PBS in each test tube was collected and replaced daily. The eluted sirolimus in the collected PBS was quantified using a high-performance liquid chromatograph (HPLC) that was equipped with a C_{18} analytic column (4.6 mm × 250 mm, particle size 5 μm, ThermoQuest, BDS, Runcorn, UK). The flow rate of the mobile phase (85% methanol, 15% deionized water, and 0.1% acetic acid by v/v), delivered by an HPLC pump (TCP, P-100, Riviera Beach, FL), was 1 mL/min at 50 ± 1 °C. The eluent was monitored using a UV detector at 254 nm.

The activity of sirolimus released from the sirolimus-loaded cylindrical or lamellar nanoarrays was evaluated using an elution test method. The test templates were well immersed in test tubes that contained a culture medium. The tubes were then incubated in a water-bath shaker at 37 °C at 120 rpm for 3 days. Subsequently, the incubated medium in each tube was collected and then applied for cell culture. RASMC (ATCC CRL-1476) (5×10^4) were seeded in a μ-Dish (35 mm, Ibidi, Martinsried, Germany) and allowed to adhere overnight. The culture medium was then replaced with fresh medium (control) or a collected medium that contained the sirolimus that was released from the cylindrical or lamellar nanoarrays. The cultures were then returned to the incubator and removed on day three for microscopic observation. The viability of the cells was evaluated according to a live/dead assay using calcein-AM and ethidium homodimer (Molecular Probes # L3224).[38]

Supporting Information Available: . Text giving detailed characterization of the sirolimus nanoarrays, AAO/sirolimus hybrids, and PS/drug blends. This material is available free of charge *via* the Internet at http://pubs.acs.org.

REFERENCES AND NOTES

1. Bates, F. S.; Fredrickson, G. H. Block Copolymer Thermodynamics: Theory and Experiment. *Annu. Rev. Phys. Chem.* **1990**, *41*, 525–557.
2. Morkved, T. L.; Lu, M.; Urbas, A. M.; Ehrichs, E. E.; Jaeger, H. M.; Mansky, P.; Russell, T. P. Local Control of Microdomain Orientation in Diblock Copolymer Thin Films with Electric Fields. *Science* **1996**, *273*, 931–933.
3. Mansky, P.; Liu, Y.; Huang, E.; Russell, T. P.; Hawker, C. Controlling Polymer-Surface Interactions with Random Copolymer Brushes. *Science* **1997**, *275*, 1458–1460.
4. Park, M.; Harrison, C.; Chaikin, P. M.; Register, R. A.; Adamson, D. H. Block Copolymer Lithography: Periodic Arrays of ~1011 Holes in 1 Square Centimeter. *Science* **1997**, *276*, 1401–1404.
5. Cheng, J. Y.; Ross, C. A.; Chan, V. Z.-H.; Thomas, E. L.; Lammertink, R. G. H.; Vancso, G. J. Formation of a Cobalt Magnetic Dot Array *via* Block Copolymer Lithography. *Adv. Mater.* **2001**, *13*, 1174–1178.
6. Temple, K.; Kulbaba, K.; Power-Billard, K. N.; Manners, I.; Leach, K. A.; Xu, T.; Russell, T. P.; Hawker, C. J. Spontaneous Vertical Ordering and Pyrolytic Formation of Nanoscopic Ceramic Patterns from Poly(styrene-*b*-ferrocenylsilane). *Adv. Mater.* **2003**, *15*, 297–300.
7. Kim, S. H.; Misner, M. J.; Xu, T.; Kimura, M.; Russell, T. P. Highly Oriented and Ordered Arrays from Block Copolymers *via* Solvent Evaporation. *Adv. Mater.* **2004**, *16*, 226–231.
8. Stoykovich, M. P.; Müller, M.; Kim, S. O.; Solak, H. H.; Edwards, E. W.; de Pablo, J. J.; Nealey, P. F. Directed Assembly of Block Copolymer Blends into Nonregular Device-Oriented Structures. *Science* **2005**, *308*, 1442–1446.
9. Ho, R. M.; Tseng, W. H.; Fan, H. W.; Chiang, Y. W.; Lin, C. C.; Ko, B. T.; Huang, B. H. Solvent-induced microdomain orientation in polystyrene-*b*-poly(L-lactide) diblock copolymer thin films for nanopatterning. *Polymer* **2005**, *46*, 9362–9377.
10. Tseng, Y. T.; Tseng, W. H.; Lin, C. H.; Ho, R. M. Fabrication of Double-Length-Scale Patterns *via* Lithography, Block Copolymer Templating, and Electrodeposition. *Adv. Mater.* **2007**, *19*, 3584–3588.
11. Thurn-Albrecht, T.; Steiner, R.; DeRouchey, J.; Stafford, C. M.; Huang, E.; Bal, M.; Tuominen, M.; Hawker, C. J.; Russell, T. P. Nanoscopic Templates from Oriented Block Copolymer Films. *Adv. Mater.* **2000**, *12*, 787–791.
12. Cheng, J. Y.; Ross, C. A.; Thomas, E. L.; Smith, H. I.; Vancso, G. J. Fabrication of nanostructures with long-range order using block copolymer lithography. *Appl. Phys. Lett.* **2002**, *81*, 3657–3659.
13. Zalusky, A. S.; Olayo-Valles, R.; Taylor, C. J.; Hillmyer, M. A. Mesoporous Polystyrene Monoliths. *J. Am. Chem. Soc.* **2001**, *123*, 1519–1520.
14. Misner, M. J.; Skaff, H.; Emrick, T.; Russell, T. P. Directed Deposition of Nanoparticles Using Diblock Copolymer Templates. *Adv. Mater.* **2003**, *15*, 221–224.
15. Johnson, B. J. S.; Wolf, J. H.; Zalusky, A. S.; Hillmyer, M. A. Template Syntheses of Polypyrrole Nanowires and CdS Nanoparticles in Porous Polymer Monoliths. *Chem. Mater.* **2004**, *16*, 2909–2917.
16. Rzayev, J.; Hillmyer, M. A. Nanoporous Polystyrene Containing Hydrophilic Pores from an ABC Triblock Copolymer Precursor. *Macromolecules* **2005**, *38*, 3–5.
17. Lo, K. H.; Tseng, W. H.; Ho, R. M. *In-Situ* Formation of CdS Nanoarrays by Pore-Filling Nanoporous Templates from Degradable Block Copolymers. *Macromolecules* **2007**, *40*, 2621–2624.
18. Zhu, B.; Zhang, Q.; Lu, Q.; Xu, Y.; Yin, J.; Hu, J.; Wang, Z. Nanotopographical Guidance of C6 Glioma Cell Alignment and Oriented Growth. *Biomaterials* **2004**, *25*, 4215–4223.
19. Nuhrenberg, T. G.; Voisard, R.; Fahlisch, F.; Rudelius, M.; Braun, J.; Gschwend, J.; Kountides, M.; Herter, T.; Baur, R.; Hombach, V.; Baeuerle, P. A.; ZohInhofer, D. Rapamycin Attenuates Vascular Wall Inflammation and Progenitor Cell Promoters after Angioplasty. *FASEB J.* **2004**, *18*, 246–248.
20. Pinchuk, L.; Wilson, G. J.; Barry, J. J.; Schoephoerster, R. T.; Parel, J. M.; Kennedy, J. P. Medical Applications of Poly(styrene-*block*-isobutylene-*block*-styrene) ("SIBS"). *Biomaterials* **2008**, *29*, 448–460.
21. Liu, L.; Guo, K.; Lu, J.; Venkatraman, S. S.; Luo, D.; Ng, K. C.; Ling, E. A.; Moochhala, S.; Yang, Y. Y. Biologically Active Core/Shell Nanoparticles Self-Assembled from Cholesterol-Terminated PEG-TAT for Drug Delivery Across the Blood-Brain Barrier. *Biomaterials* **2008**, *29*, 1509–1517.
22. Lee, C. H.; Lo, L. W.; Mou, C. Y.; Yang, C. S. Synthesis and Characterization of Positive-Charge Functionalized Mesoporous Silica Nanoparticles for Oral Drug Delivery of an Anti-Inflammatory Drug. *Adv. Funct. Mater.* **2008**, *18*, 3283–3292.
23. Jacobson, G. B.; Shinde, R.; Contag, C. H.; Zare, R. N. Sustained Release of Drugs Dispersed in Polymer Nanoparticles. *Angew. Chem., Int. Ed.* **2008**, *47*, 7880–7882.
24. Popat, K. C.; Eltgroth, M.; LaTempa, T. J.; Grimes, C. A.; Desai, T. A. Decreased *Staphylococcus epidermis* Adhesion and Increased Osteoblast Functionality on Antibiotic-Loaded Titania Nanotubes. *Biomaterials* **2007**, *28*, 4880–4888.
25. Popat, K. C.; Eltgroth, M.; La Tempa, T. J.; Grimes, C. A.; Desai, T. A. Titania Nanotubes: A Novel Platform for Drug-Eluting Coatings for Medical Implants? *Small* **2007**, *3*, 1878–1881.
26. Ko, B. T.; Lin, C. C. Synthesis, Characterization, and Catalysis of Mixed-Ligand Lithium Aggregates, Excellent Initiators for the Ring-Opening Polymerization of L-Lactide. *J. Am. Chem. Soc.* **2001**, *123*, 7973–7977.
27. Ho, R. M.; Chiang, Y. W.; Tsai, C. C.; Lin, C. C.; Ko, B. T.; Huang, B. H. Three-Dimensionally Packed Nanohelical Phase in Chiral Block Copolymers. *J. Am. Chem. Soc.* **2004**, *126*, 2704–2705.
28. Yan, M.; Harnish, B. A Simple Method for the Attachment of Polymer Films on Solid Substrates. *Adv. Mater.* **2003**, *15*, 244–248.
29. Chen, M. C.; Liang, H. F.; Chang, Y.; Chiu, Y. L.; Wei, H. J.;

Sung, H. W. A Novel Drug-Eluting Stent Spray-Coated with Multi-Layers of Collagen and Sirolimus. *J. Controlled Release* **2005**, *108*, 178–189.
30. Zalusky, A. S.; Olayo-Valles, R.; Wolf, J. H.; Hillmyer, M. A. Ordered Nanoporous Polymers from Polystyrene−Polylactide Block Copolymers. *J. Am. Chem. Soc.* **2002**, *124*, 12761–12773.
31. Yung, K. L.; Kong, J.; Xu, Y. Studies on Flow Behaviors of Polymer Melts in Nanochannels by Wetting Actions. *Polymer* **2007**, *48*, 7645–7652.
32. Siepmann, J.; Peppas, N. A. Modeling of Drug Release from Delivery Systems Based on Hydroxypropyl Methylcellulose (HPMC). *Adv. Drug Delivery Rev.* **2001**, *48*, 139–157.
33. Peng, L.; Mendelsohn, A. D.; LaTempa, T. J.; Yoriya, S.; Grimes, C. A.; Desai, T. A. Long-Term Small Molecule and Protein Elution from TiO_2 Nanotubes. *Nano Lett.* **2009**, *9*, 1932–1936.
34. Marx, S. O.; Jayaraman, T.; Go, L. O.; Marks, A. R. Rapamycin-FKBP Inhibits Cell Cycle Regulators of Proliferation in Vascular Smooth Muscle Cells. *Circ. Res.* **1995**, *76*, 412–417.
35. Fukuda, J.; Khademhosseini, A.; Yeo, Y.; Yang, X.; Yeh, J.; Eng, G.; Blumling, J.; Wang, C. F.; Kohane, D. S.; Langer, R. Micromolding of Photocrosslinkable Chitosan Hydrogel for Spheroid Microarray and Co-cultures. *Biomaterials* **2006**, *27*, 5259–5267.
36. Steinhart, M.; Wendorff, J. H.; Greiner, A.; Wehrspohn, R. B.; Nielsch, K.; Schilling, J.; Choi, J.; Gösele, U. Polymer Nanotubes by Wetting of Ordered Porous Templates. *Science* **2002**, *296*, 1997.
37. Steinhart, M.; Wehrspohn, R. B.; Gösele, U.; Wendorff, J. H. Nanotubes by Template Wetting: A Modular Assembly System. *Angew. Chem., Int. Ed.* **2004**, *43*, 1334–1344.
38. Kretsinger, J. K.; Haines, L. A.; Ozbas, B.; Pochan, D. J.; Schneider, J. P. Cytocompatibility of Self-Assembled *b*-Hairpin Peptide Hydrogel Surfaces. *Biomaterials* **2005**, *26*, 5177–5186.